Journal of Scientific Research & Reports
10(3): 1-21, 2016; Article no.JSRR.24123
ISSN: 2320-0227

SCIENCEDOMAIN *international*
www.sciencedomain.org

Unsteady MHD Flow in a Rotating Parallel Plate Channel under the Influence of Pressure Gradient with Hall Current Effects

M. Veera Krishna[1*]

[1]*Department of Mathematics, Rayalaseema University, Kurnool, Andhra Pradesh, India.*

Author's contribution

This work was carried out by only one author. Author MVK designed the Mathematical formulation of the problem and found the solution and wrote the draft of the manuscript. The author read and approved the final manuscript.

Article Information

DOI: 10.9734/JSRR/2016/24123
Editor(s):
(1) Wei-Shih Du, National Kaohsiung Normal University, Taiwan.
Reviewers:
(1) Isaac I. Animasaun, Federal University of Technology, Nigeria.
(2) Mustafa Turkyilmazoglu, University of Hacettepe, Ankara, Turkey.
(3) Sheikh Anwar Hossain, Government BL College, Khulna, Bangladesh.
(4) Mohammad Reza Safaei, University of Malaya, Malaysia.
(5) N. Sandeep, VIT University, India.
Complete Peer review History: http://sciencedomain.org/review-history/13574

Original Research Article

Received 5th January 2016
Accepted 18th February 2016
Published 5th March 2016

ABSTRACT

In this paper we discussed the unsteady flow of an incompressible electrically conducting viscous fluid in a rotating porous media, with a variable pressure gradient and in the presence of hall current. We have considered three different cases, like impulsive change, cosine and sine oscillations of pressure gradient. It is found that, the rotational and Lorentz forces are having significant effect on velocity profile in the presence of pressure gradient and hall current. The physical significance of various dimensionless parameter's are discussed analytically and numerically on velocity distribution and frictional force.

Keywords: MHD flows; unsteady flows; rotating channels; Hall current effects; pressure gradient; impulsive change; cosine oscillations and sine oscillations.

**Corresponding author: E-mail: veerakrishna_maths@yahoo.com;*

NOMENCLATURES

u : The component of the velocity along the z - axis
w : The component of the velocity along the x - axis
ρ : Fluid density
k : Permeability of the porous medium,
H_0 : Applied magnetic field,
ν : Coefficient of kinematic viscosity,
μ_e : Magnetic permeability,
P : Fluid pressure
h : Distance between the plates
E : Electric field vector
J : Current density vectors
ω_e : The cyclotron frequency
σ : The electrical conductivity of the fluid,
H : The magnetic field intensity vector,
Q : The velocity vector,
τ_e : Electron collision time,
M^2 : Hartmann number,
D : Darcy parameter (Permeability parameter),
K^2 : Rotation parameter,
Re : Reynolds number and
$f(t)$: Non-dimensional pressure gradient
$\overline{f(s)}$: Laplace transform of $f(t)$

1. INTRODUCTION

MHD flow can be used to study, assess and calculate the positions and velocities with respect to a fixed frame of reference, applying its magnetic field. The dynamics of geo-physics as a field of study has become a vital branch of fluid dynamics owing to the enormous work being carried to explore the atmosphere. MHD has extended its influence even on the studies launched in the area of astrophysics, where it is used to study the celestial occurrences like solar storms or even the dynamics working on the stellar, solar structures and the matter present between one planets and the other and between one star and the other. Hide and Roberts [1], gave an explanation for the observed continuation and secular variation of the geomagnetic field. Also Dieke [2] discussed an important in the solar physics mixed up in the sunspot development.

A phenomenon (It was discovered by Edwin Hall in 1879) that occurs when an electric current moving through a conductor is exposed to an external magnetic field applied at a right angle, in which an electric potential develops in the conductor at a right angle to both the direction of current and the magnetic field. The Hall effect was a direct result of Lorentz forces acting on the charges in the current, and was named after American physicist Edwin Herbert Hall (1855-1938). Hall current effect is also indispensable when the fluid is an ionized gas with low density or we are applying the high range of magnetic field. Because the electrical conductivity of the fluid will then be a tensor and a Hall current is provoked. Which is likely to be central in many engineering situations has been discussed by Sutton and Sherman [3]. The Hall effects on the flow of ionized gas between parallel plates under uniform transverse magnetic field have been premeditated by Sato [4]. Nanda and Mohanty [5] considered the hydromagnetic rotating channel flows. Datta and Jana [6] presented the Hall effects on unsteady Couette flow.

Hall effects on hydromagnetic convective flow through a channel with conducting walls is given by Datta and Jana [7], they discussed the flow nature with non-dimensional parameters. Mandal et al. [8] have studied the combined effects of rotation and Hall current on steady of MHD Couette flow. Mandal et al. [9] discussed

the effects of Hall current on MHD Couette flow between thick arbitrarily conducting plates. Ghosh [10] has analysed the unsteady hydromagnetic flow in a rotating channel with oscillating pressure gradient. Nagy et al. [11] discussed the effects of Hall currents and rotational force on Hartmann flow under general wall conditions. Kanch et al. [12] discussed the Hall Effect on unsteady Couette flow under boundary layer approximations. Effects of Hall current on MHD Couette flow in a rotating system with arbitrary magnetic field have been examined by Ghosh [13]. Hall effects on MHD plasma Couette flow in a rotating atmosphere have been discussed by Ghosh and Pop [14], they concluded that the hall current is significant effect on the velocity field. Ghosh [15] has been investigated the Hall effects on an MHD Couette flow in a rotating system with uninform magnetic field. Hall effects on the hydromagnetic convective flow through a rotating channel under general wall conditions have been discussed by Guria and Jana [16]. Attia [17] studied the ion-slip effects on unsteady Couette flow with heat transfer under exponential decaying pressure gradient. Seth et al. [18] have discussed the Hall effects on oscillatory hydromagnetic Couette flow in a rotating system. Hall effects on an MHD flow in a rotating channel partially filled with a porous medium have been examined by Chauhan and Rastogi [19] and Chauhan and Agrawal [20]. Jha and Apere [21] discussed the combined effects of Hall current and ion-slip current on unsteady MHD Couette flow in a rotating system. Guchhait et al. [22] have studied the combined effects of Hall current and rotation on unsteady Couette flow in a porous channel. Das et al. [23] studied Hall effects on MHD Couette flow in rotating system. Ghara et al. [24] have studied the effects of Hall current and ion-slip on unsteady MHD Couette flow. Also Seth et al. [25] investigated the effects of Hall current and rotation on unsteady MHD Couette flow in the presence of an inclined magnetic field.

Chauhan and Agrawal [26] studied the Hall effects on MHD Couette flow in a channel partially filled with a porous medium into a rotating system. Sarkar et al. [27] have examined the combined effects of Hall currents and rotation on steady hydromagnetic Couette flow. Nadeem et al. [28] discussed the numerical solutions of peristaltic flow of a Newtonian fluid under the effects of magnetic field and heat transfer in porous concentric tubes. Nadeem and Akbar [29] discussed the influence of heat transfer and variable viscosity in vertical porous annulus with peristalsis. Nadeem et al. [30] have investigated the influence of heat and mass transfer on Newtonian bio-magnetic fluid of blood flow throughout a tapered porous artery with a stenosis. Akbar and Nadeem [31] discussed the simulation of variable viscosity and Jeffrey fluid model for blood flow through a tapered artery with a stenosis. Akbar and Nadeem [32] presented the analytical and numerical analysis of Vogel's model of viscosity on the peristaltic flow of Jeffrey fluid. Das and Jana [34] discussed Hall current effects on unsteady MHD flow of viscous incompressible electrically conducting fluid through a porous channel in a rotating system with variable pressure gradient. Krishna and Irfan [36] investigated the unsteady MHD flow of Maxwell fluid through a porous medium in Rotating parallel plate channel and then extended taking hall current into account by Krishna and Irfan [35]. Krishna and Neeraja [37] discussed Hall currents on MHD flow of a couple stress fluid bounded by a porous bed in a planar channel on the lower half in occurrence of inclined magnetic field. Syamala Sarojini et al. [38] thrash out the effect of hall current on hydromagnetic flow of a couple stress fluid all the way through a porous medium in a channel in effect of inclined magnetic field. Raju et al. [39] have been studied the hall current effects on unsteady MHD three dimensional flow of a couple stress fluid through a porous medium in parallel plate channel. Recently, Krishna and Prakash [40] discussed the hall current effects on unsteady hydromagnetic flow in a parallel plate channel rotating bounded by porous bed at the lower half. Recently, the performance of unsteady non-Darcian magnetohydrodynamic fluid flow over an impulsively started vertical porous surface was investigated by Motsa and Animasaun [41]. Animasaun [42] discussed the dynamics of unsteady magnetohydrodynamic convective fluid flow with radiation and thermophoresis of particles past a vertical porous plate moving through a binary mixture in an optically thin environment. Hooman et al. [43] discussed based on slip flow at pore level a theoretical model is presented to predict the gas permeability and thereby the overall pressure drop for flow through a porous medium. Turkyilmazoglu [44] obtained explicit analytical solutions for the flow of a viscous hydromagnetic fluid due to the rotation of an infinite disk in the presence of an axial uniform steady magnetic field with Hall effects and porosity. Malvandi et al. [45] discussed MHD mixed convection *in*

a vertical annulus filled with Al_2O_3–water nano-fluid considering nanoparticle migration. Tavakoli et al. [46] study aimed at examining the cooling effect of a finned Capillary-Driven heat pipe with forced convective heat transfer on an electronic board with known heat flux. Also, the effects of size and number of fins on the heat transferred from the electronic board were studied for different power inputs. Mohidul Haque [47] discussed a numerical study of thermal diffusion effect on a mixed convective heat and mass transfer transient flow along a stretching sheet with constant heat and mass fluxes is completed under the action of a uniform magnetic field.

Motivated from the above studies, in this paper, we have considered the unsteady flow of an incompressible electrically conducting viscous fluid in the course of porous medium in a rotating system with pressure gradient as a variable and taking hall current into account.

2. FORMULATION AND SOLUTION OF THE PROBLEM

We have consider the unsteady flow of an incompressible electrically conducting viscous fluid in the course of porous medium in a rotating system between two infinitely long horizontal parallel walls separated by a distance *h* with pressure gradient as a variable and taking hall current into account. We choose a Cartesian frame of reference with the *x*-axis along the channel wall at *y* = 0. The physical configuration of the problem is as shown in Fig. 1. A uniform transverse magnetic field H_0 is applied perpendicular to the channel walls. Since the channel walls are infinite in extent and the flow is unsteady, the physical variables are the function of *y* and *t* only. The unsteady boundary layer equations for the flow through a loosely porous medium along *x* and *z*-directions in a rotating frame of reference using Brinkman model are

$$\frac{\partial u}{\partial t} - v_0 \frac{\partial u}{\partial y} + 2\Omega w = -\frac{1}{\rho}\frac{\partial p}{\partial x} + \nu \frac{\partial^2 u}{\partial y^2} - \frac{\mu_e J_z H_o}{\rho} - \frac{\nu}{k} u \quad (1)$$

$$\frac{\partial w}{\partial t} - v_0 \frac{\partial w}{\partial y} - 2\Omega u = \nu \frac{\partial^2 w}{\partial y^2} + \frac{\mu_e J_x H_o}{\rho} - \frac{\nu}{k} w \quad (2)$$

The initial and boundary conditions are

$$u = 0, w = 0, \quad t \le 0, \quad 0 \le y \le h \quad (3)$$

$$u = 0, w = 0, \quad v = v_0, \quad t > 0, \quad y = 0 \text{ and } y = h \quad (4)$$

The generalized Ohm's law comes essentially from the momentum equation of motion for the electron fluid. Its derivation can be found in some plasma physics books. It can be written, on taking Hall currents into account and neglecting ion-slip and thermo-electric effect, as (Cowling [33])

$$J + \frac{\omega_e \tau_e}{H_0}(J \times H) = \sigma\,(E + \mu_e\, q \times H) \quad (5)$$

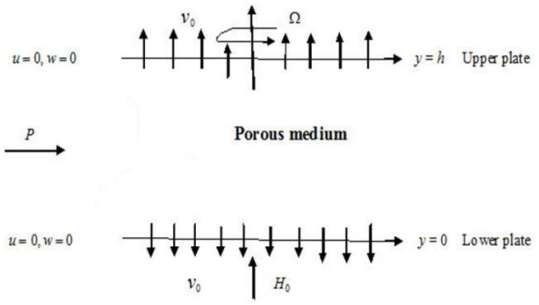

Fig. 1. Physical Geometry of the problem

The right hand side is the electric field in the moving frame. The first term on the left hand side comes from the electron drag on the ions. The second term is the Hall term and has to do with the idea that electrons and ions can decouple and move separately. The magnetic Reynolds number assumed small, so that the induced magnetic field effect is negligible in comparison with applied magnetic field. The electron atom collision frequency is relatively high as compared to the ion collision frequency, due to this the electron pressure gradient is neglected but, Hall Effect remains present. The relation $\nabla . H = 0$ for magnetic field implies $H_y = H_0 =$ constant, every-where in the fluid. Further, the equation of the conservation of the current density is $\nabla . J = 0$, gives $J_y =$ constant. This constant is zero since $J_y = 0$ at the plates which are electrically non-conducting. Thus $J_y = 0$ everywhere in the flow. Since the induced magnetic field is neglected, Maxwell's equation becomes $\nabla \times E = 0$ which implies $\frac{\partial E_x}{\partial y} = 0$ and $\frac{\partial E_z}{\partial y} = 0$. That is E_x = constant and E_z = constant everywhere in the flow. In view of the above assumption, the equation (5) gives

$$J_x - m\,J_z = -\sigma\mu_e H_0\ w \quad (6)$$

$$J_z + m\,J_x = -\sigma\mu_e H_0\ u \quad (7)$$

We solve the equations (6) and (7), and get

$$J_x = \frac{\sigma\mu_e H_0}{1+m^2}(mu - w) \quad (8)$$

$$J_z = \frac{\sigma\mu_e H_0}{1+m^2}(u + mw) \quad (9)$$

On Making use of (8) and (9), the momentum equations (1) and (2) along *x*- and *z*-directions become

$$\frac{\partial u}{\partial t} - v_0\frac{\partial u}{\partial y} + 2\Omega w = -\frac{1}{\rho}\frac{\partial p}{\partial x} + \nu\frac{\partial^2 u}{\partial y^2} + \frac{\sigma\mu_e^2 H_0^2}{\rho(1+m^2)}(u+mw) - \frac{\nu}{k}u \quad (10)$$

$$\frac{\partial w}{\partial t} - v_0\frac{\partial w}{\partial y} - 2\Omega u = \nu\frac{\partial^2 w}{\partial y^2} - \frac{\sigma\mu_e^2 H_0^2}{\rho(1+m^2)}(w - mu) - \frac{\nu}{k}w \quad (11)$$

We introduce the non-dimensional variables

$$x^* = \frac{x}{h}, y^* = \frac{y}{h}, u^* = \frac{uh}{\nu}, w^* = \frac{wh}{\nu}, q^* = \frac{qh}{\nu}, t^*. = \frac{t\nu}{h^2}, \omega^* = \frac{\omega h^2}{\nu}, p^* = \frac{ph^2}{\rho\nu^2}$$

Making use of non-dimensional variables, the equations (10) and (11) becomes to (dropping asterisks)

$$\frac{\partial u}{\partial t} - Re\frac{\partial u}{\partial y} + 2K^2 w = f(t) + \frac{\partial^2 u}{\partial y^2} - \frac{M^2}{1+m^2}(u+mw) - Du \quad (12)$$

$$\frac{\partial w}{\partial t} - Re\frac{\partial w}{\partial y} - 2K^2 u = \frac{\partial^2 w}{\partial y^2} - \frac{M^2}{1+m^2}(w - mu) - Dw \quad (13)$$

Where

$M^2 = \frac{\sigma\mu_e^2 H_0^2 h^2}{\rho\nu}$ is The Hartmann Number,

$m = \tau_e\omega_e$ the Hall Parameter,

$D = \frac{k}{h^2}$ the Darcy Parameter (Permeability Parameter),

$K^2 = \frac{\Omega^2 h^2}{\nu}$ the Rotation Parameter,

$Re = \frac{v_0 h}{\nu}$ the Reynolds Number And

$f(t) = -\frac{1}{\rho}\frac{\partial p}{\partial x}$ the Non-Dimensional Pressure Gradient.

Corresponding non-dimensional initial and boundary conditions are

$$u = 0, w = 0, \quad t \le 0, \quad 0 \le y \le 1 \quad (14)$$

$$u = 0, w = 0, \quad t > 0, \quad y = 0 \ \text{ and } \ y = 1 \quad (15)$$

Combining equations (12) and (13), Let $q = u + iw$ and $i = \sqrt{-1}$, we get the momentum equation in terms of complex velocity *q* where, *u* is the velocity along the x-direction and w is the velocity along the z-direction, is given as

$$\frac{\partial q}{\partial t} - Re\frac{\partial q}{\partial y} = f(t) + \frac{\partial^2 q}{\partial y^2} - \left(\frac{M^2}{1+im} - 2iK^2 + D \right) q \tag{16}$$

The initial and boundary conditions are

$$q = 0, \quad t \le 0, \quad 0 \le y \le 1 \tag{17}$$

$$q = 0, \quad t > 0, \quad y = 0 \ \text{ and } \ y = 1 \tag{18}$$

Taking the Laplace transform of the equation (16), we have

$$\frac{d^2\bar{q}}{dy^2} + Re\frac{d\bar{q}}{dy} - \left(\frac{M^2}{1+im} - 2iK^2 + D \right)\bar{q} = \bar{f}(s) \tag{19}$$

The transformed boundary conditions are

$$\bar{q}(0,s) = 0, \text{ and } \bar{q}(1,s) = 0 \tag{20}$$

The solution of the equation (19) subjected to the boundary conditions (20) are given by

$$\bar{q}(y,s) = \frac{\bar{f}(s)}{\lambda_1 + s}\left[1 - e^{-\frac{1}{2}\mathrm{Re}\, y}\frac{\sinh\sqrt{\lambda_2 + s}(1-y)}{\sinh\sqrt{\lambda_2 + s}} - e^{-\frac{1}{2}\mathrm{Re}(1-y)}\frac{\sinh\sqrt{\lambda_2 + s}(y)}{\sinh\sqrt{\lambda_2 + s}} \right] \tag{21}$$

Where $\lambda_1 = \frac{M^2}{1+im} - 2iK^2 + D$ and $\lambda_2 = \frac{\mathrm{Re}^2}{4} + \frac{M^2}{1+im} - 2iK^2 + D$ and we assume

$$f(t) = P_0 + P_1 e^{i\omega t} + P_2 e^{-i\omega t} \tag{22}$$

Where ω is the frequency of oscillations; P_0, P_1 and P_2 are real constants. Taking the inverse Laplace transforms to the equation (21), and we obtain the solution for the complex velocity *q* as,

$$q(y,t) = \frac{P_0}{\lambda_1}\left[1 - e^{-\frac{1}{2}\mathrm{Re}\, y}\frac{\sinh(a-ib)(1-y)}{\sinh(a-ib)} - e^{\frac{1}{2}\mathrm{Re}(1-y)}\frac{\sinh(a-ib)(y)}{\sinh(a-ib)} \right] +$$

$$\frac{P_1}{\lambda_1 + i\omega}\left[1 - e^{-\frac{1}{2}\mathrm{Re}\, y}\frac{\sinh(a_1 \pm ib_1)(1-y)}{\sinh(a_1 \pm ib_1)} - e^{\frac{1}{2}\mathrm{Re}(1-y)}\frac{\sinh(a_1 \pm ib_1)(y)}{\sinh(a_1 \pm ib_1)} \right] e^{i\omega t} +$$

$$\frac{P_2}{\lambda_1 - i\omega}\left[1 - e^{-\frac{1}{2}\mathrm{Re}\, y}\frac{\sinh(a_2 - ib_2)(1-y)}{\sinh(a_2 - ib_2)} - e^{\frac{1}{2}\mathrm{Re}(1-y)}\frac{\sinh(a_2 - ib_2)(y)}{\sinh(a_2 - ib_2)} \right] e^{-i\omega t} -$$

$$-\left(\frac{P_0}{\lambda_1} + \frac{P_1}{\lambda_1 + i\omega} + \frac{P_2}{\lambda_1 - i\omega} \right) *$$

$$\left[1-e^{-\frac{1}{2}\mathrm{Re}y}\frac{\sinh(1/2)\,\mathrm{Re}(1-y)}{\sinh(1/2)\,\mathrm{Re}}-e^{\frac{1}{2}\mathrm{Re}(1-y)}\frac{\sinh(1/2)\,\mathrm{Re}(y)}{\sinh(1/2)\,\mathrm{Re}}\right]e^{-\lambda_1 t}+$$

$$2\sum_{n=1}^{\infty}n\pi\left[(-1)^n e^{\frac{1}{2}\mathrm{Re}(1-y)}-e^{-\frac{1}{2}\mathrm{Re}(y)}\right]\left(\frac{P_0}{s_1}+\frac{P_1}{s_1+i\omega}+\frac{P_2}{s_1-i\omega}\right)\frac{\sin n\pi y}{\lambda_1+s_1}e^{s_1 t} \quad (23)$$

In the equation (23), the lower sign is valid for $2K^2+\frac{mM^2}{1+m^2}+mD>\omega$ and the upper sign is valid for $2K^2+\frac{mM^2}{1+m^2}+mD<\omega$. The equation (23) represents the velocity of the fluid in the general case. Now we shall consider the following special cases.

2.1 Velocity Distribution for Impulsive Pressure Gradient

In this case $P_1=P_2=0$, then the equation (23) reduces to

$$q(y,t)=\frac{P_0}{\lambda_1}\left[1-e^{-\frac{1}{2}\mathrm{Re}y}\frac{\sinh(a-ib)(1-y)}{\sinh(a-ib)}-e^{\frac{1}{2}\mathrm{Re}(1-y)}\frac{\sinh(a-ib)(y)}{\sinh(a-ib)}\right]+$$

$$-\frac{P_0}{\lambda_1}\left[1-e^{-\frac{1}{2}\mathrm{Re}y}\frac{\sinh(1/2)\,\mathrm{Re}(1-y)}{\sinh(1/2)\,\mathrm{Re}}-e^{\frac{1}{2}\mathrm{Re}(1-y)}\frac{\sinh(1/2)\,\mathrm{Re}(y)}{\sinh(1/2)\,\mathrm{Re}}\right]e^{-\lambda_1 t}+$$

$$+2\sum_{n=1}^{\infty}n\pi\left[(-1)^n e^{\frac{1}{2}\mathrm{Re}(1-y)}-e^{-\frac{1}{2}\mathrm{Re}(y)}\right]\left(\frac{P_0}{s_1}\right)\frac{\sin n\pi y}{\lambda_1+s_1}e^{s_1 t} \quad (24)$$

2.2 Velocity Distribution for Cosine Oscillations of Pressure Gradient

In this case $P_0=0$ and $P_1=P_2=\frac{P}{2}$, then the equation (23) reduces to

$$q(y,t)=\frac{P}{2}\left\{\left[1-e^{-\frac{1}{2}\mathrm{Re}y}\frac{\sinh(a_1\pm ib_1)(1-y)}{\sinh(a_1\pm ib_1)}-e^{\frac{1}{2}\mathrm{Re}(1-y)}\frac{\sinh(a_1\pm ib_1)(y)}{\sinh(a_1\pm ib_1)}\right]\frac{e^{i\omega t}}{\lambda_1+i\omega}+\right.$$

$$\left.\left[1-e^{-\frac{1}{2}\mathrm{Re}y}\frac{\sinh(a_2-ib_2)(1-y)}{\sinh(a_2-ib_2)}-e^{\frac{1}{2}\mathrm{Re}(1-y)}\frac{\sinh(a_2-ib_2)(y)}{\sinh(a_2-ib_2)}\right]\frac{e^{-i\omega t}}{\lambda_1-i\omega}\right\}-$$

$$-\frac{P}{2}\left(\frac{1}{\lambda_1+i\omega}+\frac{1}{\lambda_1-i\omega}\right)*$$

$$\left[1-e^{-\frac{1}{2}\mathrm{Re}y}\frac{\sinh(1/2)\,\mathrm{Re}(1-y)}{\sinh(1/2)\,\mathrm{Re}}-e^{\frac{1}{2}\mathrm{Re}(1-y)}\frac{\sinh(1/2)\,\mathrm{Re}(y)}{\sinh(1/2)\,\mathrm{Re}}\right]e^{-\lambda_1 t}+$$

$$\sum_{n=1}^{\infty}n\pi P\left[(-1)^n e^{\frac{1}{2}\mathrm{Re}(1-y)}-e^{-\frac{1}{2}\mathrm{Re}(y)}\right]\left(\frac{1}{s_1+i\omega}+\frac{1}{s_1-i\omega}\right)\frac{\sin n\pi y}{\lambda_1+s_1}e^{s_1 t} \quad (25)$$

2.3 Velocity Distribution for Sine Oscillations of Pressure Gradient

In this case $P_0 = 0$ and $P_1 = P_2 = \frac{P}{2i}$, then the equation (23) reduces to

$$q(y,t) = \frac{P}{2i}\left\{\left[1 - e^{-\frac{1}{2}\mathrm{Re}y}\frac{\sinh(a_1 \pm ib_1)(1-y)}{\sinh(a_1 \pm ib_1)} - e^{\frac{1}{2}\mathrm{Re}(1-y)}\frac{\sinh(a_1 \pm ib_1)(y)}{\sinh(a_1 \pm ib_1)}\right]\frac{e^{i\omega t}}{\lambda_1 + i\omega} + \right.$$

$$\left.\left[1 - e^{-\frac{1}{2}\mathrm{Re}y}\frac{\sinh(a_2 - ib_2)(1-y)}{\sinh(a_2 - ib_2)} - e^{\frac{1}{2}\mathrm{Re}(1-y)}\frac{\sinh(a_2 - ib_2)(y)}{\sinh(a_2 - ib_2)}\right]\frac{e^{-i\omega t}}{\lambda_1 - i\omega}\right\} -$$

$$-\frac{P}{2i}\left(\frac{1}{\lambda_1 + i\omega} + \frac{1}{\lambda_1 - i\omega}\right)^{*}$$

$$\left[1 - e^{-\frac{1}{2}\mathrm{Re}y}\frac{\sinh(1/2)\mathrm{Re}(1-y)}{\sinh(1/2)\mathrm{Re}} - e^{\frac{1}{2}\mathrm{Re}(1-y)}\frac{\sinh(1/2)\mathrm{Re}(y)}{\sinh(1/2)\mathrm{Re}}\right]e^{-\lambda_1 t} -$$

$$\sum_{n=1}^{\infty} n\pi Pi\left[(-1)^n e^{\frac{1}{2}\mathrm{Re}(1-y)} - e^{-\frac{1}{2}\mathrm{Re}(y)}\right]\left(\frac{1}{s_1 + i\omega} + \frac{1}{s_1 - i\omega}\right)\frac{\sin n\pi y}{\lambda_1 + s_1}e^{s_1 t} \qquad (26)$$

For the impulsive change of pressure gradient, the non-dimensional shear stresses at the wall $y = 0$ are given by

$$\tau_x + i\tau_z = \left(\frac{\partial q}{\partial y}\right)_{y=0} = \frac{P_0}{\lambda_1}\left[\{(1/2)\mathrm{Re} + (a - ib)\}\coth(a - ib) + \frac{\{(1/2)\mathrm{Re} - (a - ib)\}}{\sinh(a - ib)}e^{\frac{1}{2}\mathrm{Re}}\right] -$$

$$\frac{P_0\mathrm{Re}}{\lambda_1}\coth\frac{\mathrm{Re}}{2}e^{-\lambda_1 t} + 2\pi^2\ P_0\sum_{n=1}^{\infty}\left[(-1)^n e^{\frac{1}{2}\mathrm{Re}} - 1\right]\left(\frac{n^2}{s_1}\right)\frac{1}{\lambda_1 + s_1}e^{s_1 t} \qquad (27)$$

For the cosine oscillations of pressure gradient, the non-dimensional shear stresses at the wall $y = 0$ are given by

$$\tau_x + i\tau_z = \left(\frac{\partial q}{\partial y}\right)_{y=0}$$

$$= \frac{P}{2}\left\{\left[\{(1/2)\mathrm{Re} + (a_1 \pm ib_1)\}\coth(a_1 \pm ib_1) + \frac{\{(1/2)\mathrm{Re} - (a_1 \pm ib_1)\}}{\sinh(a_1 \pm ib_1)}e^{\frac{1}{2}\mathrm{Re}}\right]\frac{e^{i\omega t}}{\lambda_1 + i\omega} + \right.$$

$$\left.\left[\{(1/2)\mathrm{Re} + (a_2 - ib_2)\}\coth(a_2 - ib_2) + \frac{\{(1/2)\mathrm{Re} - (a_2 - ib_2)\}}{\sinh(a_2 - ib_2)}e^{\frac{1}{2}\mathrm{Re}}\right]\frac{e^{-i\omega t}}{\lambda_1 - i\omega}\right\}$$

$$-\frac{P\mathrm{Re}}{2}\left(\frac{1}{\lambda_1 + i\omega} + \frac{1}{\lambda_1 - i\omega}\right)\coth\left[\frac{1}{2}\mathrm{Re}\right]e^{-\lambda_1 t} +$$

$$\pi^2 P\sum_{n=1}^{\infty} n\left[(-1)^n e^{\frac{1}{2}\mathrm{Re}} - 1\right]\left(\frac{1}{s_1 + i\omega} + \frac{1}{s_1 - i\omega}\right)\frac{1}{\lambda_1 + s_1}e^{s_1 t} \qquad (28)$$

For the sine oscillations of pressure gradient, the non-dimensional shear stresses at the wall $y = 0$ are given by

$$\tau_x + i\tau_z = \left(\frac{\partial q}{\partial y}\right)_{y=0}$$

$$= \frac{P}{2i}\left\{ \left[\{(1/2)\,\mathrm{Re} + (a_1 \pm ib_1)\}\coth(a_1 \pm ib_1) + \frac{\{(1/2)\,\mathrm{Re} - (a_1 \pm ib_1)\}}{\sinh(a_1 \pm ib_1)} e^{\frac{1}{2}\mathrm{Re}} \right] \frac{e^{i\omega t}}{\lambda_1 + i\omega} + \right.$$

$$\left. \left[\{(1/2)\,\mathrm{Re} + (a_2 - ib_2)\}\coth(a_2 - ib_2) + \frac{\{(1/2)\,\mathrm{Re} - (a_2 - ib_2)\}}{\sinh(a_2 - ib_2)} e^{\frac{1}{2}\mathrm{Re}} \right] \frac{e^{-i\omega t}}{\lambda_1 - i\omega} \right\}$$

$$- \frac{P\,\mathrm{Re}}{2i}\left(\frac{1}{\lambda_1 + i\omega} + \frac{1}{\lambda_1 - i\omega} \right) \coth\left[\frac{1}{2}\mathrm{Re} \right] e^{-\lambda_1 t} +$$

$$\pi^2 P \sum_{n=1}^{\infty} n \left[(-1)^n e^{\frac{1}{2}\mathrm{Re}} - 1 \right] \left(\frac{1}{s_1 + i\omega} + \frac{1}{s_1 - i\omega} \right) \frac{1}{\lambda_1 + s_1} e^{s_1 t} \qquad (29)$$

3. RESULTS AND DISCUSSION

We have considered the unsteady flow of an incompressible electrically conducting viscous fluid in the course of porous medium in a rotating system with pressure gradient as a variable and taking hall current into account. We have computed three different cases based on our study of impulsive change, cosine and sine oscillations of pressure gradient. In this aspect, we have analytically and computationally solved the decisive equations by applying Laplace transform technique. It has been successfully established that the flow behavior is determined owing to the mutual influence of coriolis force and hydromagnetic force on each other under the purview or monitoring of pressure gradient and hall current. The flow governed by the non-dimensional parameters for the velocity components *u* and *w* with different values of magnetic parameter *M*, Hall parameter *m*, rotation parameter *K*, Reynolds number Re, *D* the permeability parameter, frequency parameter ω and phage angle ωt in Figs. (2-39). Figs. (2-11) represent the velocity profiles for impulsive pressure gradient; (12-25) represent the velocity profiles for cosine oscillations of pressure gradient, where as the Figs. (26-39) represent the velocity profiles for sine oscillations of pressure gradient. Here we observe that, all the profiles are on negative sides for *w*. Negative velocity just means velocity in the opposite direction than what would be positive. This will attained only with effect pressure gradient in pertinent directions of the flow field.

We have perceived from Figs. (2, 12 and 26) that the velocity component *u* enhances with add to Hartmann number *M* with the impulsive change of pressure gradient, and The velocity component *w* less for the cosine oscillations of while it raises with impulsive change and sine oscillations with an augment in magnetic parameter *M*, given in Figs. (3, 13 and 27). As expected due to the fact that the application of transverse magnetic field results to a resistive type force (called Lorentz force) similar to drag force and upon increasing the values of magnetic parameter, the drag force increases which leads to the deceleration of the flow. It is seen from Figs. (4, 14 and 28) that the primary velocity *u* increases with an increase in Hall parameter *m* for sine oscillations of the pressure gradient while it reduces for the impulsive change and cosine oscillations of the pressure gradient. Hence, we conclude that an increase in Hall parameter reduces the Lorentz force in *x*-direction and motion of the fluid particles is reinforced in that direction. Figs. (5, 15 and 29) shows that the secondary velocity *w* increases for the cosine and sine oscillations of the pressure gradient while it decreases for impulsive change of the pressure gradient with an increase in Hall parameter *m*. As reported in numerous MHD studies, this velocity component is a result of the Hall current effects. It is seen from Figs. (6, 7, 16, 17, 28 and 29) that the primary velocity *u* and the secondary velocity *w* decreases for cosine oscillations of the pressure gradient, while primary velocity *u* increases and *w* reduces throughout the fluid region with an increase in

rotation parameter *K* for impulse change, the reversal behaviour is observed for sine oscillations of the pressure gradient. The rotation parameter defines the relative magnitude of the Coriolis force and the viscous force in the regime; therefore it is clear that high magnitude Coriolis forces are counter-productive for the primary flow.

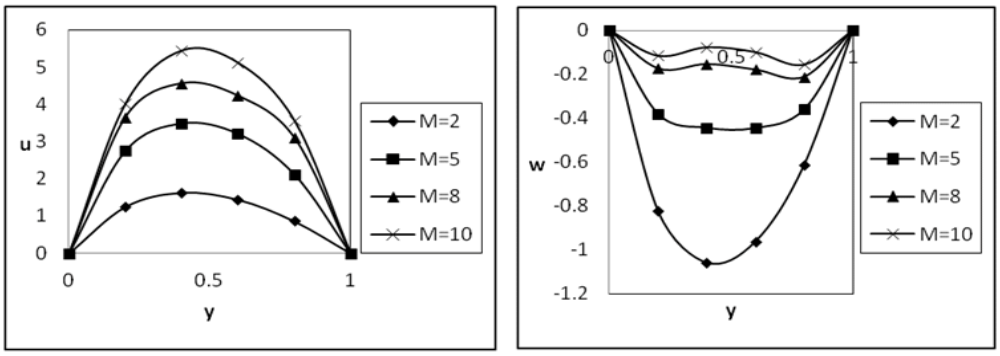

Figs. 2 and 3. The velocity profiles for *u* and *w* against *M* with
$D = 1, K = 2, \text{Re} = 2, m = 1, t = 0.1, P_0 = 10$

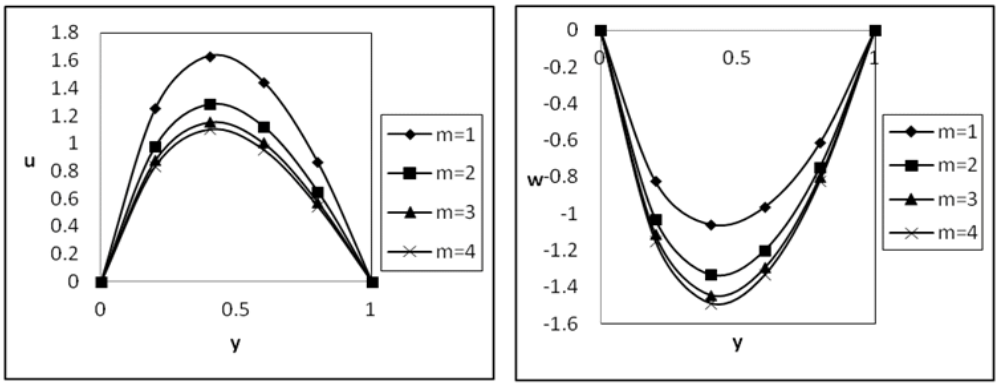

Figs. 4 and 5. The velocity profiles for *u* and *w* against *m* with
$D = 1, K = 2, \text{Re} = 2, M = 2, t = 0.1, P_0 = 10$

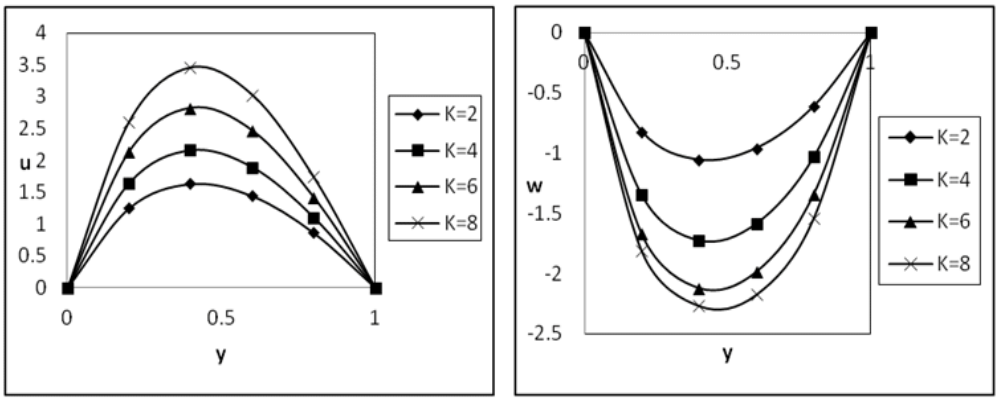

Figs. 6 and 7. The velocity profiles for *u* and *w* against *K* with
$D = 1, m = 1, \text{Re} = 2, M = 2, t = 0.1, P_0 = 10$

Figs. (8, 18 and 32), we noticed that the primary velocity *u* decreases with an increase in Reynolds number Re for the impulsive change, while it increases with an increase in Reynolds number Re for cosine oscillations of the pressure gradient, the magnitude of the velocity component *w* enhances initially for $y \le 0.2$ and then gradually reduces for $0.4 \le y \le 1$ with an increase in Reynolds number Re for sine oscillations of the pressure gradient.

From the Figs. (9, 19 and 33) it is observed that, the secondary velocity *w* increases for the impulsive change while it decreases for sine oscillations of the pressure gradient with an increase in Reynolds number Re. Similarly, the magnitude of the velocity component *w* enhances initially for $y \le 0.2$ and then gradually reduces for $0.2 < y \le 1$ with an increase in Re with cosine oscillations. It is noticed from the Figs. (10, 20 and 34) that, the primary velocity *u* amplify with an increase in permeability parameter *D* for the impulsive change, cosine and sine oscillations. Likewise from Figs. (11, 21 and 35) that the secondary velocity *w* reduces with an increase in permeability parameter *D* for sine oscillations while it raises for impulsive change and cosine oscillations. The primary velocity *u* increases with ω for cosine oscillations, whereas the velocity *u* develops for $\omega = 2, 4 \,\&\, 6$ and then experiences retardation for $\omega = 8$, sine oscillations given Figs. (22 and 36). It is also observed from the Figs. (23 and 37), the magnitude of the secondary velocity *w* diminishes for the sine oscillations while *u* enhances for $\omega = 2, 4 \,\&\, 6$ and then experiences retardation for $\omega = 8$ with cosine oscillations with raise in frequency parameter ω.

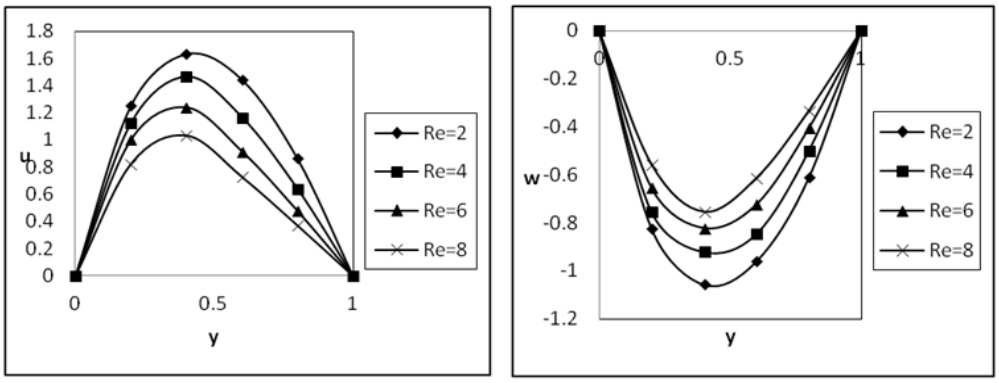

Figs. 8 and 9. The velocity profiles for *u* and *w* against Re with
$D = 1, K = 2, M = 2, m = 1, t = 0.1, P_0 = 10$

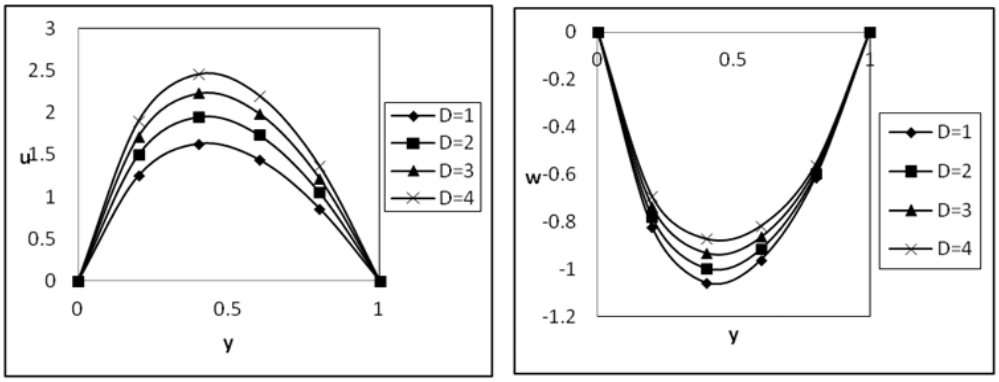

Figs. 10 and 11. The velocity profiles for *u* against *D* with
$\mathrm{Re} = 2, K = 2, M = 2, m = 1, t = 0.1, P_0 = 10$

Finally we have noticed from Figs. (24 and 38) that, the magnitude of the primary velocity *u* decreases with an increase in phase angle ωt for both cosine and sine oscillations of the pressure gradient. From Figs. (25 and 39), we noticed that the magnitude of the secondary velocity *w* diminishes for cosine oscillations of the pressure gradient while it raises for sine oscillations of the pressure gradient with increase in phase angle ωt . The magnitudes of the velocities for cosine are more effective than sine oscillations of the pressure gradient. The best results are obtained to compare with Das et al. [23, 24 & 34]. The results are coincide with Das and Jana [34] when $D,\ m \to 0$. Hall effect and variable pressure gradient shown the impact on the primary and secondary velocity of the fluid flow and verified for *m* tends to zero.

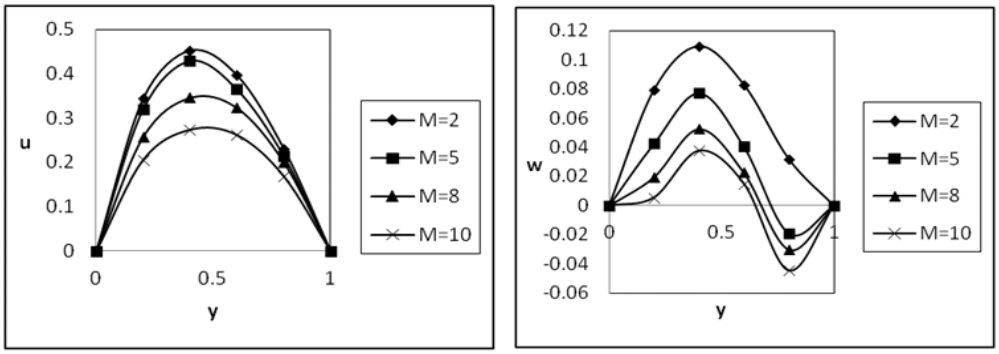

Figs. 12 and 13. The velocity profiles for *u* and *w* against *M* with
$D = 1, K = 2,\ \mathrm{Re} = 2, m = 1, \omega = 2, \omega t = \pi/4,\ t = 0.1, P_1 = P_2 = 5$

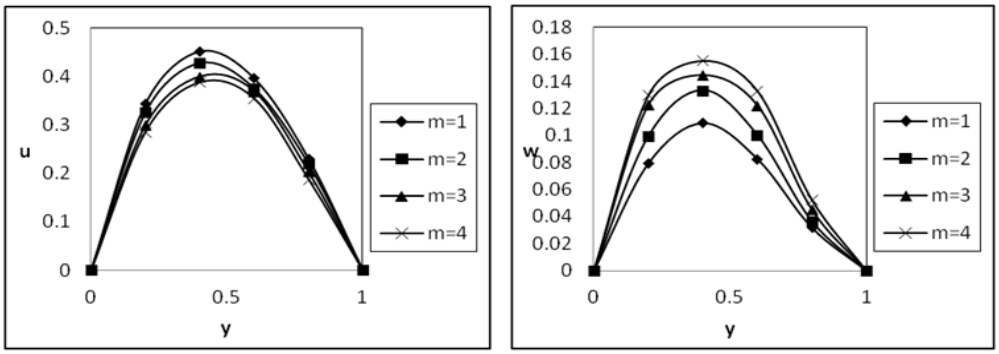

Figs. 14 and 15. The velocity profiles for *u* and *w* against *m* with
$D = 1, K = 2,\ \mathrm{Re} = 2, M = 2, \omega = 2, \omega t = \pi/4, t = 0.1, P_1 = P_2 = 5$

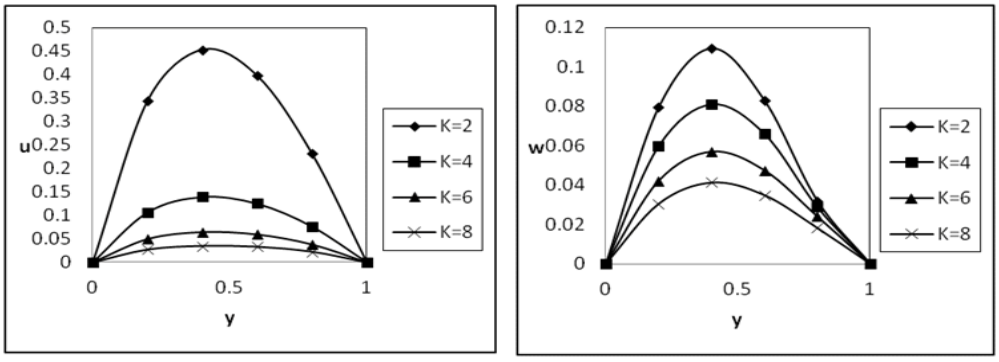

Fig. 16 and 17. The velocity profiles for *u* and *w* against *K* with
$D = 1, m = 1,\ \mathrm{Re} = 2, M = 2, \omega = 2, \omega t = \pi/4,\ t = 0.1, P_1 = P_2 = 5$

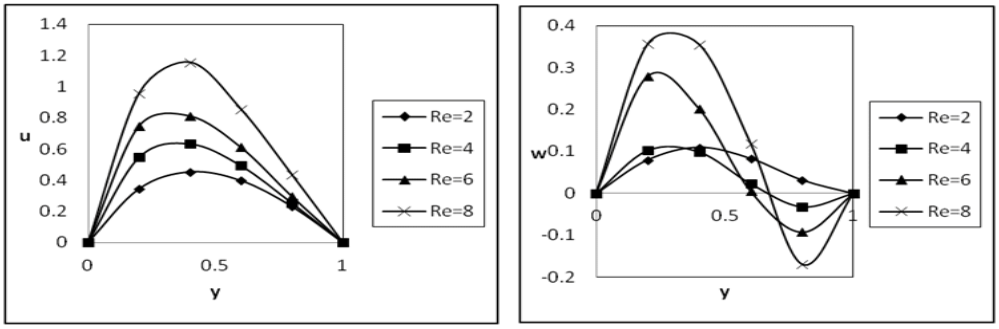

Figs. 18 and 19. The velocity profiles for *u* and *w* against Re with

$D = 1, K = 2, M = 2, m = 1, \omega = 2, \omega t = \pi / 4, t = 0.1, P_1 = P_2 = 5$

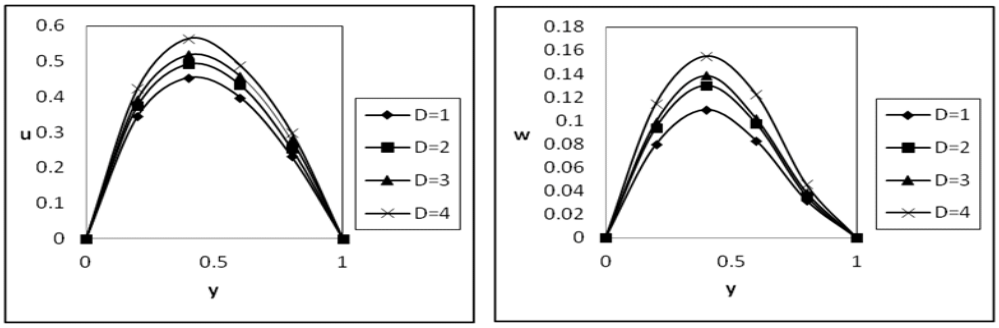

Figs. 20 and 21. The velocity Profiles for *u* and *w* against *D* with

$\mathrm{Re} = 2, K = 2, M = 2, m = 1, \omega = 2, \omega t = \pi / 4, t = 0.1, P_1 = P_2 = 5$

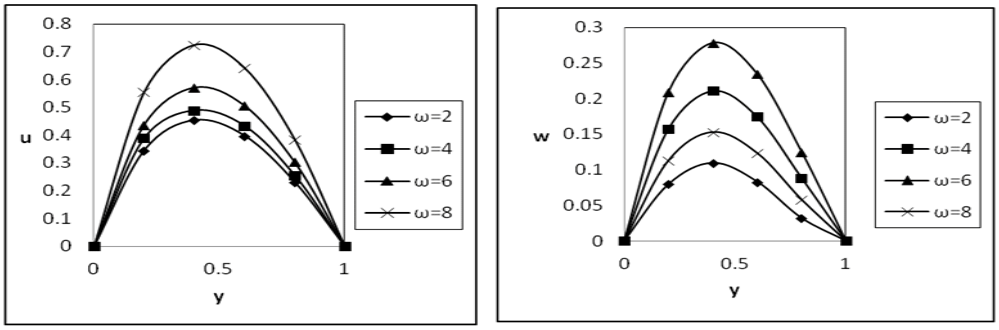

Figs. 22 and 23. The velocity Profiles for *u* and *w* against ω with

$\mathrm{Re} = 2, K = 2, D = 1, M = 2, m = 1, \omega t = \pi / 4, t = 0.1, P_1 = P_2 = 5$

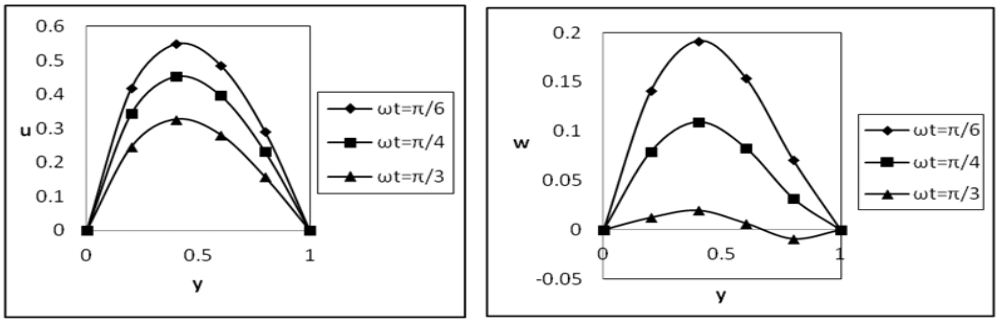

Figs. 24 and 25. The velocity profiles for *u* and *w* against ωt with

$\mathrm{Re} = 2, K = 2, M = 2, m = 1, \omega = 2, t = 0.1, P_1 = P_2 = 5$

The non-dimensional shear stresses τ_x and τ_z have been calculated at the wall ($y = 0$) due to the primary and the secondary flows are presented in Tables (1-3) and computationally discussed with reference to governing parameters. We notice that the shear stresses τ_x and τ_z due to the primary and secondary flow at the wall $y = 0$ reduce for the impulsive change, cosine and sine oscillations of the pressure gradient with raise in *M*. The shear stress τ_x due to the primary flow at the wall $y = 0$ reduces for both impulsive change and cosine oscillations while it enhances for sine oscillations of the pressure gradient with raise in hall parameter *m*. The magnitude of the shear stress τ_z due to the secondary flow at the wall $y = 0$ increases for the impulsive change, cosine and sine oscillations of the pressure gradient with an augment in *m*. The magnitude of the shear stress τ_x due to the primary flow diminishes for the impulsive change and cosine oscillations. Also it enhances for sine oscillations of the pressure gradient with add to in *K* or *D*. It is found that the shear stress τ_z decreases for both impulsive change and cosine oscillations of the pressure gradient while it increases for sine oscillations of the pressure gradient with an increase in *K* and *D*. The magnitude of the shear stress τ_x reduces for small values of magnetic parameter *M* and then it enhances for the impulsive change, cosine and sine oscillations of the pressure gradient with an increase in Re. The magnitude of the shear stress τ_z enhances for both impulsive change and cosine oscillations of the pressure gradient while it decreases for sine oscillations of the pressure gradient with an increase in Re. The shear stress τ_x enhances for small values of *M* and then it decreases for cosine and sine oscillations of the pressure gradient with a raise in frequency parameter ω.

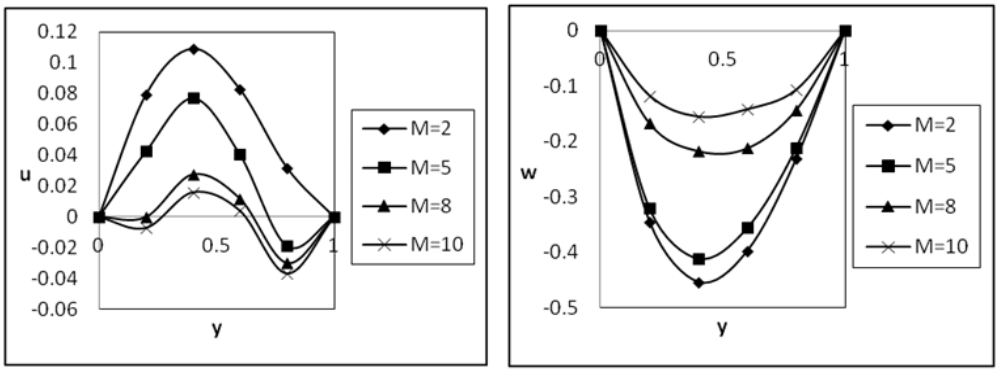

Figs. 26 and 27. The velocity profiles for *u* and *w* against *M* with
$D = 1, K = 2, \text{Re} = 2, m = 1, \omega = 2, \omega t = \pi / 4, t = 0.1, P_1 = P_2 = 5$

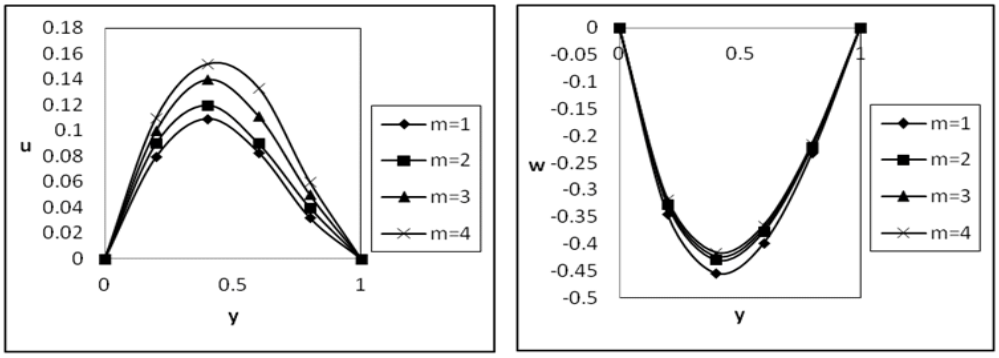

Figs. 28 and 29. The velocity profiles for *u* and *w* against *m* with
$D = 1, K = 2, \text{Re} = 2, M = 2, \omega = 2, \omega t = \pi / 4, t = 0.1, P_1 = P_2 = 5$

The shear stress τ_z enhances for small values of magnetic parameter *M* and then it decreases for cosine oscillations while opposite nature for sine oscillations of the pressure gradient with an increase in ω. The shear stress τ_x diminishes for both cosine and sine oscillations with increment in phase angle ωt. The shear stress τ_z decreases for cosine oscillations and increases for sine oscillations for enhancement in phase angle ωt.

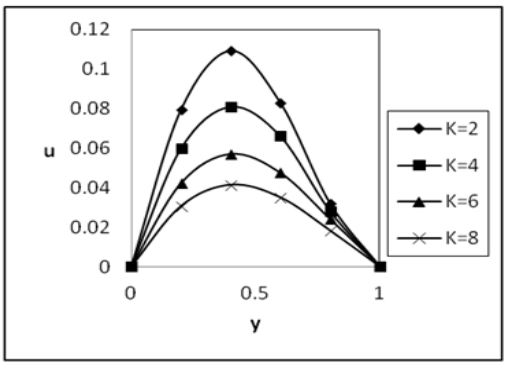

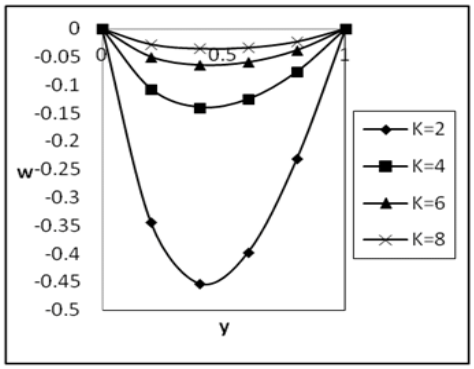

Figs. 30 and 31. The velocity profiles for *u* and *w* against *K* with
$D = 1, m = 1, \text{Re} = 2, M = 2, \omega = 2, \omega t = \pi/4, t = 0.1, P_1 = P_2 = 5$

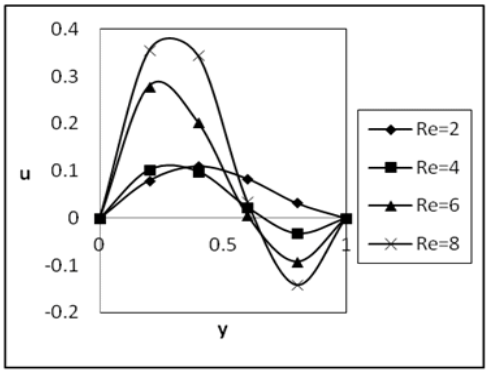

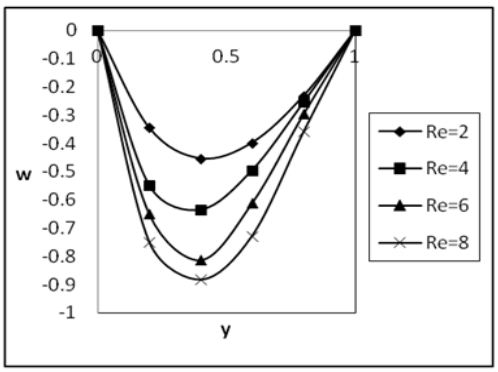

Figs. 32 and 33. The velocity profiles for *u* and *w* against Re with
$D = 1, K = 2, M = 2, m = 1, \omega = 2, \omega t = \pi/4, t = 0.1, P_1 = P_2 = 5$

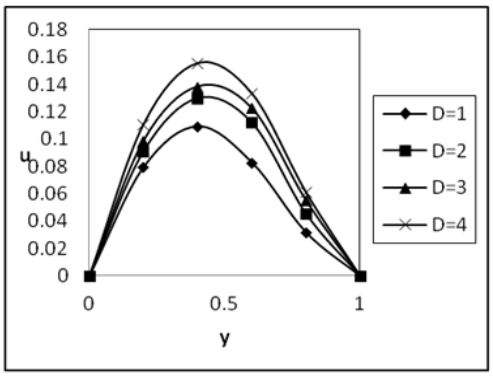

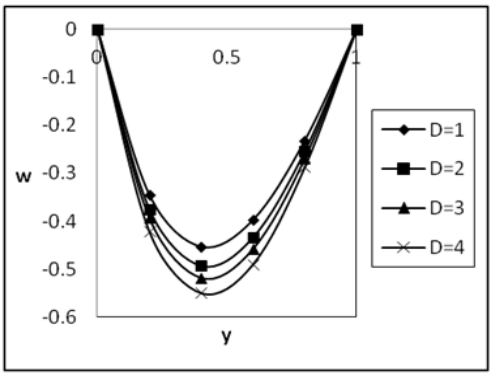

Figs. 34 and 35. The velocity profiles for *u* and *w* against *D* with
$\text{Re} = 2, K = 2, M = 2, m = 1, \omega = 2, \omega t = \pi/4, t = 0.1, P_1 = P_2 = 5$

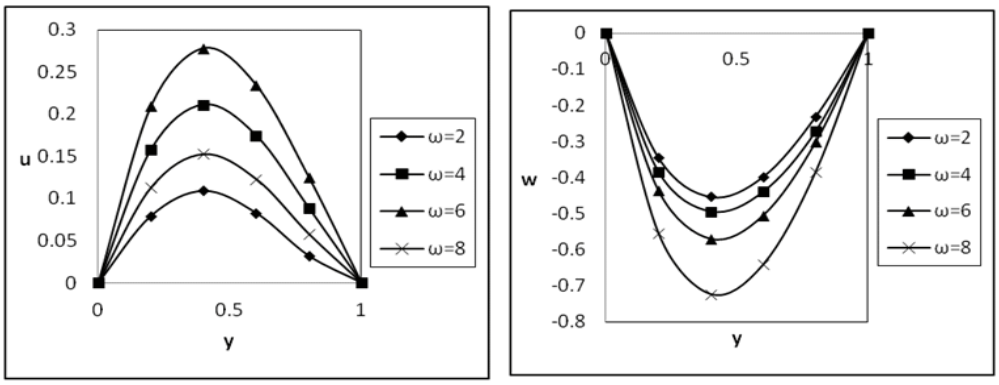

Figs. 36 and 37. The velocity profiles for *u* and *w* against ω with $\mathrm{Re} = 2, K = 2, D = 1, M = 2, m = 1, \omega t = \pi/4, t = 0.1, P_1 = P_2 = 5$

Table 1. The shear stresses at the wall $y = 0$ with impulsive pressure gradient

M	*m*	*K*	Re	*D*	τ_x	τ_z
2	**1**	**2**	**2**	**1**	0.920545	0.566585
5	1	2	2	1	0.755471	0.510225
8	1	2	2	1	0.544854	0.478845
2	**2**	2	2	1	0.844758	0.655482
2	**3**	2	2	1	0.744855	0.685956
2	1	**4**	2	1	0.901254	0.522142
2	1	**6**	2	1	0.887459	0.500214
2	1	2	**4**	1	0.785540	0.788548
2	1	2	**6**	1	0.678801	0.966569
2	1	2	2	**2**	0.855852	0.704458
2	1	2	2	**3**	0.648878	0.800145

Table 2. The shear stresses at the wall $y = 0$ with cosine oscillations of pressure gradient

M	*m*	*K*	Re	*D*	ω	ωt	τ_x	τ_z
2	**1**	**2**	**2**	**1**	**2**	$\pi/4$	0.814025	0.662152
5	1	2	2	1	2	$\pi/4$	0.755845	0.622154
8	1	2	2	1	2	$\pi/4$	0.681452	0.596655
2	**2**	2	2	1	2	$\pi/4$	0.755845	0.688542
2	**3**	2	2	1	2	$\pi/4$	0.700122	0.665225
2	1	**4**	2	1	2	$\pi/4$	0.722459	0.604252
2	1	**6**	2	1	2	$\pi/4$	0.622546	0.541125
2	1	2	**4**	1	2	$\pi/4$	0.788458	0.725546
2	1	2	**6**	1	2	$\pi/4$	0.688982	0.788544
2	1	2	2	**2**	2	$\pi/4$	0.699885	0.755066
2	1	2	2	**3**	2	$\pi/4$	0.588987	0.822103
2	1	2	2	1	**4**	$\pi/4$	0.998702	0.702254
2	1	2	2	1	**6**	$\pi/4$	1.225473	0.722546
2	1	2	2	1	2	$\pi/6$	0.885442	0.622352
2	1	2	2	1	2	$\pi/3$	0.745582	0.600214

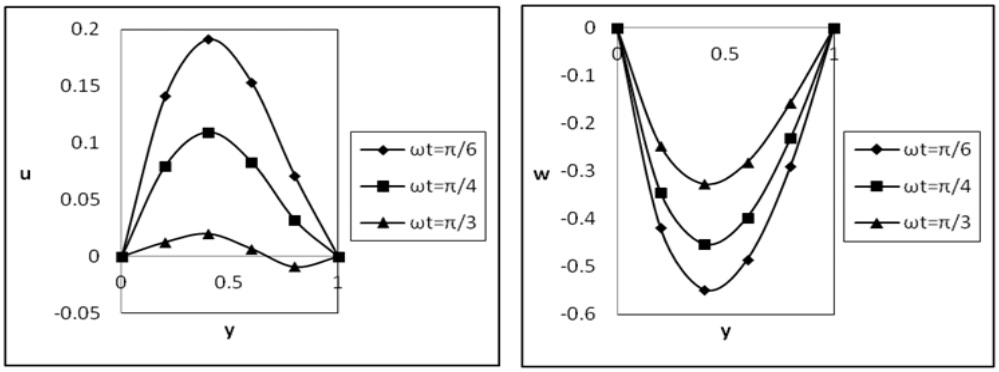

Figs. 38 and 39. The velocity profiles for *u* and *w* against ωt with
$\mathrm{Re} = 2, K = 2, M = 2, m = 1, \omega = 2, t = 0.1, P_1 = P_2 = 5$

Table 3. The shear stresses at the wall $y = 0$ with sine oscillations of pressure gradient

M	*m*	*K*	Re	*D*	ω	ωt	τ_x	τ_z
2	**1**	**2**	**2**	**1**	**2**	$\pi/4$	0.356636	0.278843
5	1	2	2	1	2	$\pi/4$	0.322546	0.255655
8	1	2	2	1	2	$\pi/4$	0.299555	0.233652
2	**2**	2	2	1	2	$\pi/4$	0.366526	0.288548
2	**3**	2	2	1	2	$\pi/4$	0.377458	0.299666
2	1	**4**	2	1	2	$\pi/4$	0.388546	0.296585
2	1	**6**	2	1	2	$\pi/4$	0.399658	0.322145
2	1	2	**4**	1	2	$\pi/4$	0.321021	0.222541
2	1	2	**6**	1	2	$\pi/4$	0.301332	0.201145
2	1	2	2	**2**	2	$\pi/4$	0.366525	0.325266
2	1	2	2	**3**	2	$\pi/4$	0.377785	0.350021
2	1	2	2	1	**4**	$\pi/4$	0.255466	0.254025
2	1	2	2	1	**6**	$\pi/4$	0.221455	0.313365
2	1	2	2	1	2	$\pi/6$	0.422515	0.352662
2	1	2	2	1	2	$\pi/3$	0.333256	0.399685

4. CONCLUSIONS

We have considered the unsteady flow of an incompressible electrically conducting viscous fluid in the course of porous medium in a rotating system with pressure gradient as a variable and taking hall current into account. The conclusions are made as follows.

1. The velocity component for primary flow enhances with increasing *M*, *K* and *D*, and reduces with *m*, Re for the impulsive change of pressure gradient.
2. The velocity component for secondary flow enhances with increasing *M*, Re and *D*, and reduces with *m* and *K* for the impulsive change of pressure gradient.
3. The velocity component for primary flow increases with increasing Re, *D* and ω, and reduces with *M*, *m*, *K* and phase angle ωt for the cosine oscillations of pressure gradient.
4. The velocity for primary flow increases with increasing *m* and *D*, and reduces with *M*, *K* and phase angle ωt for the sine oscillations of pressure gradient.
5. The magnitude of the velocity for primary flow and for secondary flow enhances initially and then gradually reduces with an increase in Reynolds number Re for sine and cosine oscillations of the pressure gradient respectively.
6. The velocity for secondary flow enhances with increasing *M*, *m*, *K* and phase angle ωt, and reduces with increase in Re, *D* and frequency of oscillation ω for the impulsive change of pressure gradient.

7. The magnitude of τ_x due to the primary flow decreases for the impulsive change and cosine oscillations with increment in *M*, *m*, Re, *K* and *D*. For secondary flow it reduces for K and *M* and increases for *m*, Re and *D*.
8. Both the stresses enhance with increase in *m*, *K* and *D*; and reduce with increase in *M* or Re for sine of the pressure gradient.
9. The shear stress τ_x increases for petite values of *M* and then it reduces for cosine and sine oscillations of the pressure gradient with an increase in frequency parameter ω.
10. The stress τ_z enhances and then it reduces for cosine oscillations. Whereas it initially decreases and then boosts for sine oscillations of the pressure gradient with an increase in ω.
11. Finally, the rotational and Lorentz forces are having significant effect on velocity profile in the presence of pressure gradient and hall current.

ACKNOWLEDGEMENTS

The authors are thankful to Prof. Y. Nara simhulu, Vice-Chanceller, Rayalaseema Uni versity, Kurnool, and Prof. R. Siva Prasad, Department of Mathematics, Sri Krishna Devaraya University, Anantapur, Andhra Pradesh, India, and this journal for the support to develop this document.

COMPETING INTERESTS

Author has declared that no competing interests exist.

REFERENCES

1. Hide R, Roberts PH. The origin of the mean geomagnetic field. In: Physics and Chemistry of the Earth. Pergamon Press, New York. 1961;4:27-98.
2. Dieke RH. Internal rotation of the sun. In: Goldberg L, (Ed.), Annual Reviews of Astronomy and Astrophysics. Annual Reviews Inc. 1970;8:297-328.
3. Sutton GW, Sherman A. Engineering magneto hydro dynamics. Mc Graw-Hill, New York; 1965.
4. Sato H. The Hall effects in the viscous flow of ionized gas between parallel plates under transverse magnetic field. Journal of Phys. Soc. Japan. 1961;16:14-27.
5. Nanda RS, Mohanty HK. Hydro magnetic rotating channel flows. Appl. Sci. Res. A. 1970;24:65-75.
6. Datta N, Jana RN. Hall effects on unsteady Couette flow. International Journal of Engineering Sciences. 1977;15:35-43.
7. Datta N, Jana RN. Hall effects on hydro magnetic convective flow through a channel with conducting walls. Inter-national Journal of Engineering Sciences. 1977;15:561-572.
8. Mandal G, Mandal KK, Choudhury G. On combined effects of Coriolis force and Hall current on steady MHD Couette flow and heat transfer. Journal of Phys. Soc. Japan. 1982;51:2010-2015.
9. Mandal G, Mandal KK. Effects of Hall current on MHD Couette flow between thick arbitrarily conducting plates in a rotating system. Journal of Phys. Soc. Japan. 1983;52:470.
10. Ghosh SK. Unsteady hydro magnetic flow in a rotating channel with oscillating pressure gradient. Journal of Phys. Soc. Japan. 1993;62:893-3903.
11. Nagy T, Demandy Z. Effects of Hall currents and Coriolis force on Hartmann flow under general wall conditions. Acta Mechanica. 1995;113:77-91.
12. Kanch AK, Jana RN. Hall effect on unsteady Couette flow under boundary layer approximations. Journal of Physical Sciences. 2001;7:74-86.
13. Ghosh SK. Effects of Hall current on MHD Couette flow in a rotating system with arbitrary magnetic field. Czech. J. Phys. 2002;52:51-63.
14. Ghosh SK, Pop I. Hall effects on MHD plasma Couette flow in a rotating environment. International Journal of Applied Mechanical Engineering. 2004; 9(2):293-305.
15. Ghosh SK. Effects of Hall current on MHD Couette flow in a rotating system with arbitrary magnetic field. Czech. J. Phys. 2002;52(1):51-63.
16. Guria M, Jana RN. Hall effects on the hydro magnetic convective flow through a rotating channel under general wall conditions. Magneto Hydro Dynamics. 2007;43(3);287-300.
17. Attia HA. Ion slip effects on unsteady Couette flow with heat transfer under exponential decaying pressure gradient.

Tamkang Journal and Engineering. 2009;12(2):209-214.

18. Seth GS, Nandkeolyar R, Ansari MdS. Hall effects on oscillatory hydromagnetic Couette flow in a rotating system. International Journal of Acad. Res. 2009;1: 6.
19. Chauhan DS, Rastogi P. Hall current and heat transfer effects on MHD flow in a channel partially filled with a porous medium in a rotating system. Turkish Journal of Engineering & Environmental Sciences. 2009;33:167-184.
20. Chauhan DS, Agrawal R. Effects of Hall current on MHD flow in a rotating channel partially filled with a porous medium. Chemical Engineering Communications. 2010;197(6):830-845.
21. Jha BK, Apere CA. Combined effects of Hall current and ion-slip current on unsteady MHD Couette flow in a rotating system. Journal of Physical Society of Japan. 2010;79(10):104401(1-9).
22. Guchhait SK, Das S, Jana RN, Ghosh SK. Combined effects of Hall current and rotation on unsteady Couette flow in a porous channel. World Journal of Mechanics. 2011;1:87-99.
23. Das S, Sarkar BC, Jana RN. Hall effects on MHD Couette flow in rotating system. International Journal of Computer Applications. 2011;35(13):22-30.
24. Ghara N, Maji SL, Das S, Jana RN, Ghosh SK. Effects of Hall current and ion-slip on unsteady MHD Couette flow. Open Journal of Fluid Dynamics. 2012;2:1-13.
25. Seth GS, Nandkeolyar R, Ansari MdS. Effects of Hall current and rotation on unsteady MHD Couette flow in the presence of an inclined magnetic field. Journal of Applied Fluid Mechanics. 2012;5(2):67-74.
26. Chauhan DS, Agrawal R. Effects of hall current on MHD Couette flow in a channel partially filled with a porous medium in a rotating system. Meccanica. 2012;47:405-421.
27. Sarkar BC, Das S, Jana RN. Combined effects of Hall currents and rotation on steady hydro magnetic Couette flow. Research Journal of Applied Sciences, Engineering and Technology. 2013;5(6): 1864-1875.
28. Nadeem S, Akbar NS, Malik MY. Numerical solutions of peristaltic flow of a newtonian fluid under the effects of magnetic field and heat transfer in a porous concentric tubes. Zeitschrift fur Naturforschung. 2010;65a(5):369-380.
29. Nadeem S, Akbar NS. Influence of heat transfer and variable viscosity in vertical porous annulus with peristalsis. Journal of Porous Media. 2011;14:849-863.
30. Nadeem S, Akbar NS, Hayat T, Hendi AA. Influence of heat and mass transfer on Newtonian biomagnetic fluid of blood flow through a tapered porous arteries with a stenosis. Transport in Porous Media. 2012;91:81-100.
31. Akbar NS, Nadeem S. Simulation of variable viscosity and Jeffrey fluid model for blood flow through a tapered artery with a stenosis. Communications in Theoretical Physics. 2012;57:133-140.
32. Akbar NS, Nadeem S. Analytical and numerical analysis of Vogel's model of viscosity on the peristaltic flow of Jeffrey fluid. Journal of Aerospace Engineering. 2012;25:64-71.
33. Cowling TG. Magneto hydro dynamics, New York, Intersscience; 1957.
34. Das S, Rabindra Nath Jana. Hall effects on unsteady MHD flow through a porous channel in a rotating system with variable pressure gradient" (chapter), Ph.D thesis, Department of Applied Mathematics, Vidyasagar University, Midnapore, India.
35. Veera Krishna M, Md Irfan Ahmed. Hall effect on unsteady MHD flow of Maxwell fluid through a porous medium in Rotating parallel plate channel. International Journal of Applied Mathematics and Engineering Sciences. 2014;8(1):11-27.
36. Veera Krishna M, Md Irfan Ahmed. Unsteady MHD flow of Maxwell fluid through a porous medium in Rotating parallel plate channel. International Journal of Applied Mathematical Analysis and Applications. 2014;9(2):97-115.
37. Veera Krishna M, Neeraja E. Hall currents on MHD flow of a couple stress fluid in a parallel plate channel bounded by a porous bed on the lower half in presence of inclined magnetic field. International Journal of Advanced Technology and Engineering Research. 2013;3(3):103-114.
38. Syamala Sarojini M, Veera Krishna M, Uma Shankar C. Effects of hall currents on MHD flow of a couple stress fluid through a porous medium in a parallel plate channel in presence of effect of inclined magnetic

field. International Journal of Dynamics of Fluids. 2012;8(2):67-78.

39. Raju G, Veera Krishna M, Siva Prasad R. Hall current effects on unsteady MHD three dimensional flow of a couple stress fluid through a porous medium in parallel plate channel. International Journal of Physics and Mathematical Sciences. 2013; 3(1):18-31.
40. Veera Krishna M, Prakash J. Hall current effects on Unsteady MHD flow in a Rotating parallel plate channel bounded by Porous bed on the Lowerhalf - Darcy Lapwood model. Open Journal of Fluid Dynamics. 2015;5:275-294. Available:http://dx.doi.org/10.4236/ojfd.2015.54029
41. Sandile Sydney Motsa, Isaac L Animasaun. A new numerical investigation of some thermo-physical properties on unsteady MHD Non-Darcian flow past an impulsively started vertical surface. Thermal Science. 2015;19(Suppl. 1):S249-S258.
42. Animasaun. Dynamics of unsteady MHD convective flow with thermophoresis of particles and variable thermo - Physical properties past a vertical surface moving through binary mixture. Open Journal of Fluid Dynamics. 2015;5,106-120. Available:http://dx.doi.org/10.4236/ojfd.2015.52013
43. Hooman K, Tamayol A, Dahari M, Safaei MR, Togun H, Sadri R. A theoretical model to predict gas permeability for slip flow through a porous medium. Applied Thermal Engineering. 2014;70:71-76. Available:http://dx.doi.org/10,1016/j.applthermaleng.2014.04.071
44. Turkyilmazoglu. Exact solutions for the incompressible viscous magnetohydro dynamic fluid of a porous rotating disk flow with Hall current. International Journal of Mechanical Sciences. 2012;56(1):86-95. Available:http://dx.doi.org/10.1016/j.ijmecsci.2012.01.008
45. Malvandin A, Safaei MR, Kaffash MH, Ganji DD. MHD mixed convection in a vertical annulus filled with Al2O3-water nanofluid considering nanoparticle migration. Journal of Magnetism and Magnetic Materials. 2015;382:296-306. Available:http://dx.doi.org/10.1016/j.jmmmm.2015.01.060
46. Mohammad Reza Tavakoli, Reza Zaghian, Ali Mohammadi. Application of heat pipes with forced convective heat transfer in cooling of electronic equipments. Journal of Scientific Research and Reports. 2015;8(1):1-9. Available:http://dx.doi.org/10.9734/JSRR/2015/18420
47. Md. Mohidul Haque, Ujjal Kumar Sarder. Thermal diffusion effect on convective heat and mass transfer of high speed mhd flow over a stretching sheet. Journal of Scientific Research and Reports. 2015; 8(1):1-14. Available:http://dx.doi.org/10.9734/JSRR/2015/18075

APPENDIX

$$s_1 = -\left(n^2\pi^2 + \frac{Re^2}{4} + \frac{M^2}{1+im} - 2iK^2 + D \right)$$

$$a = \frac{1}{\sqrt{2}} \left[\left\{ \left(\frac{Re^2}{4} + \frac{M^2}{1+m^2} + D \right)^2 + \left(2K^2 + \frac{mM^2}{1+m^2} + mD \right)^2 \right\}^{1/2} + \left(\frac{Re^2}{4} + \frac{M^2}{1+m^2} + D \right) \right]^{1/2}$$

$$b = \frac{1}{\sqrt{2}} \left[\left\{ \left(\frac{Re^2}{4} + \frac{M^2}{1+m^2} + D \right)^2 + \left(2K^2 + \frac{mM^2}{1+m^2} + mD \right)^2 \right\}^{1/2} - \left(\frac{Re^2}{4} + \frac{M^2}{1+m^2} + D \right) \right]^{1/2}$$

$$a_1 = \frac{1}{\sqrt{2}} \left[\left\{ \left(\frac{Re^2}{4} + \frac{M^2}{1+m^2} + D \right)^2 + \left(2K^2 + \frac{mM^2}{1+m^2} + mD - \omega \right)^2 \right\}^{1/2} + \left(\frac{Re^2}{4} + \frac{M^2}{1+m^2} + D \right) \right]^{1/2}$$

$$b_1 = \frac{1}{\sqrt{2}} \left[\left\{ \left(\frac{Re^2}{4} + \frac{M^2}{1+m^2} + D \right)^2 + \left(2K^2 + \frac{mM^2}{1+m^2} + mD - \omega \right)^2 \right\}^{1/2} - \left(\frac{Re^2}{4} + \frac{M^2}{1+m^2} + D \right) \right]^{1/2}$$

$$a_2 = \frac{1}{\sqrt{2}} \left[\left\{ \left(\frac{Re^2}{4} + \frac{M^2}{1+m^2} + D \right)^2 + \left(2K^2 + \frac{mM^2}{1+m^2} + mD + \omega \right)^2 \right\}^{1/2} + \left(\frac{Re^2}{4} + \frac{M^2}{1+m^2} + D \right) \right]^{1/2}$$

$$b_2 = \frac{1}{\sqrt{2}} \left[\left\{ \left(\frac{Re^2}{4} + \frac{M^2}{1+m^2} + D \right)^2 + \left(2K^2 + \frac{mM^2}{1+m^2} + mD + \omega \right)^2 \right\}^{1/2} - \left(\frac{Re^2}{4} + \frac{M^2}{1+m^2} + D \right) \right]^{1/2}$$

Peer-review history:
The peer review history for this paper can be accessed here:
http://sciencedomain.org/review-history/13574